Journal of Engineering Mathematics, Vol. 13, No. 2, April 1979

Analytical and numerical results for the non-stationary rotating disk flow

H. SCHIPPERS

Philips Research Laboratories, Eindhoven, The Netherlands *

(Received September 5, 1978)

SUMMARY

This paper deals with the time-dependent flow due to an infinite rotating disk. The Navier-Stokes equations are transformed by Von Kármán's similarity approach. The resulting equations have been studied both numerically and analytically for two cases: (1) the flow due to a disk whose angular velocity abruptly changes sign, and (2) the oscillating disk flow. Some numerical results are compared with the outcome of the analysis.

1. Introduction

In the present paper the time-dependent flow caused by an infinite rotating disk is investigated. Problems of this kind have received much attention in the literature. Most of the solutions found are of the Von Kármán class, describing the stationary flow. Von Kármán found in 1921 that the equations of motion were accessible for similarity solutions, i.e. the radial and tangential velocities vary linearly with radius r, whereas the axial velocity depends only on the distance z to the disk. The present paper is restricted to discussing this category of solutions.

The time-dependent problem has been studied both numerically and analytically. Solutions of the former type have been obtained by Pearson ([1], [2]), Florent et al. ([3], [4]), Bodonyi and Stewartson [5] and Homsy and Hudson [6]; they all used finite difference techniques. Analytical solutions are found in the literature in the form of series expansions. Riley [7], Benney [8] and Rosenblat [9] have examined the flow caused by a disk oscillating in an infinite medium. For a given angular velocity $\Omega \cos\omega t$ of the disk they developed a solution in the form of a power series in terms of the dimensionless parameter $\epsilon = \Omega/\omega$. Rosenblat and Benney examined the high-frequency flow ($\epsilon \ll 1$); Riley also studied the low-frequency case ($\epsilon \gg 1$).

Benton [10] has studied the flow caused by an impulsively starting disk in an infinite medium. For the velocity field he gives series expansions in terms of the angle of rotation Ωt.

In the present paper two cases are considered: (1) the intermittently rotating disk, i.e. the flow due to a rotating disk whose angular velocity abruptly changes sign, and (2) the oscillating disk for several regimes of the parameter ϵ. The following subjects will be discussed. In Section 2 the differential equations and boundary conditions for this type of problems are presented.

* Present address: Mathematical Center, 2e Boerhaavestr. 49, 1091 AL Amsterdam, The Netherlands.

Section 3 deals with two numerical computational methods, which are based on Zandbergen's and Dijkstra's numerical approach [11]. In Section 4 the analytical results are extended and compared with the numerical solutions. The results of the work described here allow a few conclusions to be drawn, which are summarized in Section 5.

The stimulus for the present study came from the interest of Philips Research Laboratories in an industrial application of intermittently rotating disks.

2. Basic equations

The basic equations for the incompressible, viscous flow are the Navier-Stokes and continuity equations, which can be reduced by means of the Von Kármán similarity transformations to

$$F_t = F_{zz} - HF_z - F^2 + G^2 - K, \tag{2.1}$$

$$G_t = G_{zz} - HG_z - 2FG, \tag{2.2}$$

$$2F + H_z = 0, \tag{2.3}$$

where (F, G, H) and K are a measure of the velocity vector and radial pressure gradient respectively in a cylindrical polar coordinate system (r, ϕ, z). The dimensionless time t is a measure of the angle of rotation. A fourth equation serves to determine the axial pressure gradient after the velocity components have been found. This equation has been omitted. The boundary conditions are given by the no-slip conditions. Assuming that an infinite disk rotates in the plane $z = 0$, they are:

$$F(0, t) = H(0, t) = 0, \qquad G(0, t) = g(t). \tag{2.4}$$

In our applications the function $g(t)$ is a block function for the intermittently rotating disk and $\cos(\epsilon^{-1} t)$ for the oscillating disk. Further we need conditions at infinity. Assuming that the radial and azimuthal components of the velocity tend to zero (here only axial inflow is possible), we get:

$$F(\infty, t) = G(\infty, t) = 0. \tag{2.5}$$

It can be shown that $K(t) = G^2(\infty, t)$.

This problem involves two relevant length scales:

1. Von Kármán layer thickness $(\nu/\Omega)^{\frac{1}{2}}$, where ν is the kinematic viscosity,
2. Stokes layer thickness $(\nu/\omega)^{\frac{1}{2}}$.

It will be apparent that the oscillating disk flow is characterized by the parameter $\epsilon = \Omega/\omega$, which determines the ratio of the Stokes layer to the Von Kármán layer thickness.

3. Numerical approach

Numerical methods have been used, which are based on the approach given by Zandbergen and Dijkstra [11] for the stationary rotating disk flow. Finite difference techniques are applied to problem formulation (2.1) – (2.3). In calculations the boundary conditions (2.5) are applied at a finite value $z = z_m$:

$$F(z_m) = G(z_m) = 0.$$

The choice of z_m depends on the required accuracy.

If we want to resolve the flow structure near to the disk with a limited number of mesh points, it appears to be necessary to transform the z-coordinate in a suitable way. Let us map $[0, z_m]$ into the new range $[0, 1]$ by means of a mapping ϕ. Thus $z = \phi(x)$, where x is an element of the new range. We denote the inverse function of ϕ by ψ.

The mesh covering the new range $0 \leqslant x \leqslant 1$ is uniform with the stepsize Δx and the mesh points x_j are given by

$$\Delta x = 1/N, \qquad x_j = j\Delta x, \qquad j = 0(1)N.$$

In cases where the angular velocity of the rotating disk is abruptly changed it is advisable to introduce another scale of time $s = s(t)$, taking into account the discontinuity of the velocity of that disk.

Let $F_{j,k}$ be the value of $F(x, s)$ at mesh point $x = x_j$ and at the time $s = s_k$. The right-hand sides of (2.1) – (2.2) are now discretized by central differences at $s = s_k$. The non-stationary term is approximated by two different backward-difference formulae:

$$F_s = (F_{j,k} - F_{j,k-1})/\Delta s, \tag{3.1}$$

$$F_s = (3F_{j,k} - 4F_{j,k-1} + F_{j,k-2})/(2\Delta s), \tag{3.2}$$

in which $\Delta s = s_k - s_{k-1}$ is the uniform time step.

Using this approach and formula (3.1) we get a system of finite difference equations, which is called the fully implicit method (F.I.). The system which arises after applying formula (3.2) is referred to as the three-point backward implicit method (B3). The disadvantage of the F.I. method is that it is of order $O(\Delta s, \Delta x^2)$. The B3 method is of the order $O(\Delta s^2, \Delta x^2)$, but difficulties arise in starting it: at the point $s = s_1$ we do not have values at $s = s_{-1}$. In our numerical calculations we use the F.I. method to start B3.

If we choose the F.I. method for solving (2.1) – (2.2) and integrate (2.3) using the trapezoidal rule we get a system of finite difference equations for the quantities $H_{j,k}$, $G_{j,k}$ and $F_{j,k}$. In the equations below we have taken:

$$T(s) = \frac{dt}{ds}(s), \qquad P(x) = \psi_z(z(x)), \qquad Q(x) = \psi_{zz}(z(x)),$$

and from the eqs. (2.1) – (2.3) we thus obtain:

$$P_j(H_{j,k} - H_{j-1,k}) + \Delta x(F_{j-1,k} + F_{j,k}) = 0, \quad \text{for } j = 1(1)N, \tag{3.3}$$

$$G_{j,k} - G_{j,k-1} - T_k \frac{\Delta s}{\Delta x^2} (P_j^2(G_{j+1,k} - 2G_{j,k} + G_{j-1,k}) + \tag{3.4}$$

$$+ \frac{\Delta x}{2} (Q_j - P_j H_{j,k})(G_{j+1,k} - G_{j-1,k}) - 2\Delta x^2 F_{j,k} G_{j,k}) = 0,$$

$$\text{for } j = 1(1)N - 1,$$

$$F_{j,k} - F_{j,k-1} - T_k \frac{\Delta s}{\Delta x^2} (P_j^2(F_{j+1,k} - 2F_{j,k} + F_{j-1,k}) + \tag{3.5}$$

$$+ \frac{\Delta x}{2} (Q_j - P_j H_{j,k})(F_{j+1,k} - F_{j-1,k}) - \Delta x^2 F_{j,k}^2 + \Delta x^2 G_{j,k}^2) = 0,$$

$$\text{for } j = 1(1)N - 1.$$

A method of solving this system of 3N – 2 non-linear algebraic equations by means of Newton iteration has been given by Zandbergen and Dijkstra [11]. This approach leads to a linear system of equations for the Newton corrections. The bandwidth of the system is seven and the matrix routine takes advantage of this property.

4. Single-disk problems

In this section the analytical results of Benton [10] and Benney [8] are extended to allow us to judge the numerical results. Two cases are discussed: in Section 4.1. the intermittently rotating disk flow and in Section 4.2 the oscillating disk flow.

4.1. Intermittently rotating disk

The flow induced by an impulsively started disk was considered by Benton [10], who was given exact representations of the non-steady velocity field by power series in the angle of rotation Ωt.

Using the technique of matched asymptotic expansions we give in Section 4.1.1 series for the flow induced by a rotating disk, whose angular velocity abruptly changes sign. In Section 4.1.2 the numerical results found with the approach given in Section 3 are compared with the outcome of the series expansions.

4.1.1. Analytical results

Matched asymptotic expansions are used to study the flow induced by a rotating disk whose angular velocity abruptly changes sign. Just before the change of direction of disk rotation at time $t = 0$ the stationary Von Kármán flow prevails. Thus the initial conditions are:

$$F(z,0) = \bar{F}(z), \qquad G(z,0) = \bar{G}(z), \qquad H(z,0) = \bar{H}(z),$$

where $\bar{F}$, $\bar{G}$ and $\bar{H}$ are given by the Von Kármán solution. The disk is now made to rotate in the opposite sense. A time-dependent inner layer then grows at the surface of the disk. Furthermore there is still the Von Kármán boundary layer. This, in fact, makes it necessary to split the velocity components, i.e., $F(z, t) = \bar{F}(z) + \tilde{F}(z, t)$. Similar relations apply to G and H and substituting these into (2.1) – (2.3) we obtain:

$$\tilde{F}_t = \tilde{F}_{zz} - \bar{H}\tilde{F}_z - \tilde{H}\bar{F}_z - \tilde{H}\tilde{F}_z - (\tilde{F}^2 + 2\tilde{F}\bar{F}) + (\tilde{G}^2 + 2\tilde{G}\bar{G}), \tag{4.1}$$

$$\tilde{G}_t = \tilde{G}_{zz} - \bar{H}\tilde{G}_z - \tilde{H}\bar{G}_z - \tilde{H}\tilde{G}_z - 2(\tilde{F}\tilde{G} + \bar{F}\tilde{G} + \tilde{F}\bar{G}), \tag{4.2}$$

$$\tilde{H}_z + 2\tilde{F} = 0. \tag{4.3}$$

The initial and boundary conditions are respectively:

$$\tilde{F}(z, 0) = \tilde{H}(z, 0) = \tilde{G}(z, 0) = 0 \tag{4.4}$$

and

$$\tilde{F}(0, t) = \tilde{F}(\infty, t) = \tilde{H}(0, t) = \tilde{G}(\infty, t) = 0, \tag{4.5}$$

$$\tilde{G}(0, t) = \begin{cases} 0 & \text{for } t = 0, \\ -2 & \text{if } t > 0. \end{cases}$$

The coordinate in the inner layer is given by $\eta = z/2\sqrt{t}$ and the velocity components are defined as $\hat{F}(\eta, t) = \tilde{F}(z, t)$, $\hat{G}(\eta, t) = \tilde{G}(z, t)$ and $\hat{H}(\eta, t) = \tilde{H}(z, t)$. Just after the reversal of the disk rotation the inner layer is much thinner than the Von Kármán layer, and therefore we can approximate $\bar{H}$, $\bar{G}$ and $\bar{F}$ by their Taylor series expansions. After substitution we get the following equations:

$$\hat{H}_\eta + 4\sqrt{t}\hat{F} = 0, \tag{4.6}$$

$$\begin{aligned} \hat{G}_{\eta\eta} + 2\eta\hat{G}_\eta - 4t\hat{G}_t = {} & 2\sqrt{t}\left\{2\eta^2 t\bar{H}''(0) + \frac{8}{3}\eta^3 t^{3/2} + O(t^2)\right\}\hat{G}_\eta + \\ & + 4t\hat{H}\{\bar{G}'(0) - 2\eta^2 t\bar{H}''(0) + O(t^{3/2})\} + 2\sqrt{t}\hat{H}\hat{G}_\eta + 8t\hat{F}\hat{G} + \\ & + 8t\hat{G}\left\{-\eta\sqrt{t}\bar{H}''(0) - 2\eta^2 t - \frac{8}{3}\bar{G}'(0)\eta^3 t^{3/2} + O(t^2)\right\} + \\ & + 8t\hat{F}\left\{1 + 2\eta\sqrt{t}\bar{G}'(0) - \frac{4}{3}\eta^3 t^{3/2}\bar{H}''(0) + O(t^2)\right\}, \end{aligned} \tag{4.7}$$

$$\begin{aligned} \hat{F}_{\eta\eta} + 2\eta\hat{F}_\eta - 4t\hat{F}_t = {} & 2\sqrt{t}\left\{2\eta^2 t\bar{H}''(0) + \frac{8}{3}\eta^3 t^{3/2} + O(t^2)\right\}\hat{F}_\eta + \\ & + 4t\hat{H}\left\{-\frac{1}{2}\bar{H}''(0) - 2\eta\sqrt{t} - 4\bar{G}'(0)\eta^2 t + O(t^{3/2})\right\} + 2\sqrt{t}\hat{H}\hat{F}_\eta + 4t\hat{F}^2 + \\ & + 8t\hat{F}\left\{-\eta\sqrt{t}\bar{H}''(0) - 2\eta^2 t - \frac{8}{3}\bar{G}'(0)\eta^3 t^{3/2} + O(t^2)\right\} - 4t\hat{G}^2 + \\ & - 8t\hat{G}\left\{1 + 2\eta\sqrt{t}\bar{G}'(0) - \frac{4}{3}\eta^3 t^{3/2}\bar{H}''(0) + O(t^2)\right\}. \end{aligned} \tag{4.8}$$

From the literature the values of $\bar{H}''(0)$ and $\bar{G}'(0)$ are known to be respectively -1.02046 and -0.61592. Following Benton [10] we can perform series expansions involving powers of $\sqrt{t}$ with coefficients which are functions of the inner variable η:

$$\hat{G}(\eta, t) = G_0(\eta) + t^{3/2} G_1(\eta) + t^2 G_2(\eta) + \ldots,$$
$$\hat{F}(\eta, t) = tF_1(\eta) + t^{3/2} F_2(\eta) + t^{5/2} F_3(\eta) + \ldots,$$
$$\hat{H}(\eta, t) = -4t^{1/2} \{tH_1(\eta) + t^{3/2} H_2(\eta) + t^{5/2} H_3(\eta) + \ldots\}$$

The difference from the Benton series is caused by the presence of the Von Kármán solution in the equations of motion (4.1) and (4.2) Substitution of our series into (4.6) – (4.8) leads to a hierarchy of ordinary differential equations for G_0, F_1, H_1, etc. In [12] we determined exact solutions for these functions:

$$G_0(\eta) = -2 \operatorname{erfc} \eta,$$
$$F_1(\eta) = 4\left(1 + \frac{2}{\pi}\right)\left\{(1 + 2\eta^2)\operatorname{erfc} \eta - \frac{2}{\sqrt{\pi}} \eta e^{-\eta^2}\right\} +$$
$$- 8\left\{\eta \operatorname{erfc} \eta - \frac{1}{\sqrt{\pi}} e^{-\eta^2}\right\}^2 - 4 \operatorname{erfc} \eta,$$
$$G_1(\eta) = \frac{1}{6} \bar{H}''(0)\left\{\frac{-18}{\sqrt{\pi}} \eta^2 e^{-\eta^2} + (10\eta^3 - 9\eta)\operatorname{erfc} \eta\right\},$$
$$F_2(\eta) = -2\bar{G}'(0)\left\{\frac{2}{\sqrt{\pi}} \eta^2 e^{-\eta^2} - (2\eta^3 - \eta)\operatorname{erfc} \eta\right\}.$$

The functions H_1 and H_2 are obtained by a single integration of F_1 and F_2 respectively. In particular we obtain:

$$H_1(\eta) = \frac{4}{3}\left(1 + \frac{2}{\pi}\right)\left\{(3\eta + 2\eta^3)\operatorname{erfc} \eta - \frac{2}{\sqrt{\pi}}(1 + \eta^2)e^{-\eta^2}\right\} +$$
$$- \frac{8}{3} \eta\left\{\frac{1}{\sqrt{\pi}} e^{-\eta^2} - \eta \operatorname{erfc} \eta\right\}^2 - \frac{8}{3\sqrt{\pi}} e^{-\eta^2} \operatorname{erfc} \eta + \frac{8}{3}\left(\frac{2}{\pi}\right)^{\frac{1}{2}} \operatorname{erfc} \sqrt{2}\eta +$$
$$- 4\eta \operatorname{erfc} \eta + \frac{4}{\sqrt{\pi}} e^{-\eta^2} + \frac{8}{3\sqrt{\pi}}\left(\frac{2}{\pi} - \sqrt{2} + \frac{1}{2}\right),$$
$$H_2(\eta \to \infty) \sim -\frac{3}{4} \bar{G}'(0).$$

Proceeding with the determination of $F_3(\eta)$ we encounter a major difficulty: it appears to be impossible to choose the integration constants such that $F_3(\infty) = 0$. This points to a perturbation of the outer flow, which is related to the axial velocity at the edge of the inner layer, i.e.:

$$\hat{H}(\infty, t) \sim \frac{-32}{3\sqrt{\pi}}\left(\frac{2}{\pi} - \sqrt{2} + \frac{1}{2}\right) t^{3/2} + 3\bar{G}'(0) t^2. \tag{4.9}$$

This mechanism is responsible for the change of the outer Von Kármán layer. Hence there must be an outer expansion describing this process. The coordinates in the outer layer are z and t. Introducing outer layer components of velocity $\dot{H}$, $\dot{G}$ and $\dot{F}$, we see that the expansions in this layer are determined by the condition that the inner must be matched to the outer solution for small values of t. Therefore it is necessary to start the expansion for $\dot{H}$ with a term $t^{3/2}$, while $\dot{F}$ and $\dot{G}$ begin with $t^{5/2}$:

$$\dot{H}(z,t) = t^{3/2}h_1(z) + t^2 h_2(z) + t^{5/2}h_3(z) + t^3 h_4(z) + O(t^{7/2}),$$
$$\dot{G}(z,t) = t^{5/2}g_1(z) + t^3 g_2(z) + t^{7/2}g_3(z) + O(t^4),$$
$$\dot{F}(z,t) = t^{5/2}f_1(z) + t^3 f_2(z) + t^{7/2}f_3(z) + O(t^4).$$

Substitution of these series into (4.1) – (4.3) leads to the following system of equations for h_1, f_1, g_1, etc.:

$$h_1' = 0, \tag{4.10}$$
$$\frac{5}{2} f_1 = -h_1 \bar{F}_z, \tag{4.11}$$
$$\frac{5}{2} g_1 = -h_1 \bar{G}_z, \tag{4.12}$$
$$h_2' = 0, \tag{4.13}$$
$$3f_2 = -h_2 \bar{F}_z, \tag{4.14}$$
$$3g_2 = -h_2 \bar{G}_z, \tag{4.15}$$
$$h_3' = -2f_1, \tag{4.16}$$
$$\frac{7}{2} f_3 = f_1'' - \bar{H}f_1' - h_3 \bar{F}_z - 2\bar{F}f_1 + 2\bar{G}g_1, \tag{4.17}$$
$$\frac{7}{2} g_3 = g_1'' - \bar{H}g_1' - h_3 \bar{G}_z - 2\bar{F}g_1 - 2\bar{G}f_1, \tag{4.18}$$
$$h_4' = -2f_2. \tag{4.19}$$

To verify our numerical results we are interested in $H(\infty, t)$ and $H_{zz}(0,t)$. Therefore we only determine h_1, f_1, h_2, f_2, h_3 and h_4. The boundary conditions at $z = 0$ follow from the matching of the inner to the outer expansion. From (4.9) it will be clear that

$$h_1(z) \equiv \frac{-32}{3\sqrt{\pi}}\left(\frac{2}{\pi} - \sqrt{2} + \frac{1}{2}\right),$$
$$h_2(z) \equiv 3\bar{G}'(0).$$

From (4.11) and (4.14) it is easily seen that

$$f_1(z) = \frac{-32}{15\sqrt{\pi}}\left(\frac{2}{\pi} - \sqrt{2} + \frac{1}{2}\right)\bar{H}_{zz}(z),$$

$$f_2(z) = \frac{1}{2}\,\bar{G}'(0)\bar{H}_{zz}(z).$$

The boundary conditions $F_3(0) = 0$ and $F_3(\infty) = f_1(0)$ determine $F_3(\eta)$ to be

$$\begin{aligned} F_3(\eta) \;=\; & H''(0)\left(\frac{7}{15\pi} - \frac{115}{48}\right)\left\{(4\eta^5 + 20\eta^3 + 15\eta)\operatorname{erfc}\eta + \right. \\ & \left. - (4\eta^4 + 18\eta^2 + 8)\frac{1}{\sqrt{\pi}}e^{-\eta^2}\right\} - \frac{32}{15}\bar{H}''(0)\left(\frac{2}{\pi}\right)^{\frac{1}{2}}\operatorname{erfc}\sqrt{2}\,\eta + \\ & + 8\bar{H}''(0)\left\{\frac{11}{20}\eta^5 + \frac{31}{12}\eta^3 + \frac{37}{16}\eta\right\}\operatorname{erfc}^2\eta + \\ & + 8\bar{H}''(0)\left\{\left(\frac{5}{12} - \frac{4}{3\pi}\right)\eta^3 + \left(\frac{1}{8} - \frac{1}{\pi}\right)\eta + \right. \\ & \left. - \frac{1}{\sqrt{\pi}}\left(\frac{11}{10}\eta^4 + \frac{499}{120}\eta^2 + \frac{161}{80}\right)e^{-\eta^2}\right\}\operatorname{erfc}\eta + \\ & + 8\bar{H}''(0)\left[\frac{1}{\pi}\left(\frac{11}{20}\eta^3 + \frac{63}{40}\eta\right)e^{-2\eta^2} + \frac{1}{\sqrt{\pi}}\left\{\left(\frac{4}{3\pi} - \frac{7}{12}\right)\eta^2 + \right.\right. \\ & \left.\left. + \left(\frac{1}{\pi} - \frac{1}{4}\right)\right\}e^{-\eta^2} - \frac{4}{15\sqrt{\pi}}\left(\frac{2}{\pi} - \sqrt{2} + \frac{1}{2}\right)\right]. \end{aligned}$$

A single integration of $F_3(\eta)$ gives

$$H_3(\eta \to \infty) \sim \frac{-32}{15\sqrt{\pi}}\bar{H}''(0)\left(\frac{2}{\pi} - \sqrt{2} + \frac{1}{2}\right)\eta + \bar{H}''(0)\left(\frac{335}{192} - \frac{29}{4\pi}\right).$$

From the matching of the inner to the outer expansion and taking account of eqs. (4.16) and (4.19) it follows that

$$h_3(z) = \frac{64}{15\sqrt{\pi}}\left(\frac{2}{\pi} - \sqrt{2} + \frac{1}{2}\right)H_z(z),$$

$$h_4(z) = -\bar{G}'(0)\bar{H}_z(z) + \bar{H}''(0)\left(\frac{29}{\pi} - \frac{335}{48}\right).$$

These results allow us to calculate $H_{zz}(0, t)$ and $H(\infty, t)$ as:

$$\begin{aligned} H_{zz}(0,t) = \; & \bar{H}''(0) + \frac{8}{\sqrt{\pi}}\left(\frac{4}{\pi} - 1\right)t^{1/2} + 2\bar{G}'(0)t + \\ & + \left(\frac{263}{16} - \frac{157}{3\pi}\right)\bar{H}''(0)t^2 + O(t^{5/2}), \end{aligned} \tag{4.20}$$

$$H(\infty, t) = \bar{H}(\infty) - \frac{32}{3\sqrt{\pi}} \left(\frac{2}{\pi} - \sqrt{2} + \frac{1}{2}\right) t^{3/2} + 3G'(0)t^2 + \tag{4.21}$$
$$+ H''(0) \left(\frac{29}{\pi} - \frac{335}{48}\right) t^3 + O(t^{7/2}).$$

4.1.2. Numerical results

Numerical results are obtained using the approach given in Section 3. The main errors are: (a) cut-off error, which arises from fixing infinity at a certain value, and (b) discretization errors. The fully implicit method (F.I.) yields $O(\Delta s, \Delta x^2)$, while the B3 method results in $O(\Delta s^2, \Delta x^2)$.

In order to take account of the diffusion of the inner layer into the Von Kármán layer we have scaled time by $t = s^2$. The range $0 \leqslant z \leqslant z_m$ (with $z_m = 10$) is divided into N uniform meshes. The shear stress at the disk (i.e. H_{zz}) is determined by numerical differentiation.

In the intermittently rotating disk flow we are interested in the results just after the reversal of the disk. The F.I. method is used and the numerical results are extrapolated.

The effect of the spatial Richardson extrapolation (based on Δz^2) is illustrated in the following table, which presents results obtained with $\Delta s = \frac{1}{32}\sqrt{2\pi}$.

TABLE 1

Effect of the spatial Richardson extrapolation for the intermittently rotating disk flow using the F.I. method.

Δz	$H_{zz}(0, \pi/8)$	Extrapolation	
1/4	−0.575847		
1/8	−0.650645	−0.675578	
1/16	−0.673255	−0.680792	−0.681139

The same can be done with the results obtained with $\Delta s = \frac{1}{16}\sqrt{2\pi}, \frac{1}{8}\sqrt{2\pi}$. We get three extrapolated values for $H_{zz}(0, \pi/8)$. These results are used for illustrating the Richardson extrapolation in time (based on Δs) as is shown in Table 2:

TABLE 2

Effect of Richardson extrapolation in time for the intermittently rotating disk flow using the F.I. method.

Δs	$H_{zz}(0, \pi/8)$	Extrapolation	
$\frac{1}{8}\sqrt{2\pi}$	−0.659946		
$\frac{1}{16}\sqrt{2\pi}$	−0.673630	−0.687314	
$\frac{1}{32}\sqrt{2\pi}$	−0.681139	−0.688648	−0.689093

In Table 3 the extrapolated results for some values of t are presented and compared with the outcome of (4.20).

TABLE 3

Comparison between numerical and analytical results $H_{zz}(0, t)$ for the intermittently rotating disk flow using the F.I. method.

Time	Numerical	Analytical	Difference
0	−1.0200	−1.0205	0.0005
$\pi/32$	−0.7506	−0.7528	0.0022
$\pi/8$	−0.6891	−0.6967	0.0076
$9\pi/32$	−0.7550	−0.7739	0.0189
$\pi/2$	−0.8613	−0.8543	0.0070
$25\pi/32$	−0.9467	−0.7554	0.1913

Inspection of this table reveals a discrepancy of $O(\Delta t)$ between the numerical and analytical results for small values of t, which requires further investigation.

It should be remarked that the analytical results have been obtained by adding terms of different order $O(t^{1/2})$, $O(t)$ and $O(t^2)$. For a particular case the various terms are:

$\bar{H}_{zz}(0)$	1st term	2nd term	3rd term	$H_{zz}(0, \pi/8)$
−1.0205	0.7728	−0.4838	0.0347	−0.6967

In order to investigate the quality of the fully implicit method we also compare the numerical results for the axial inflow with the outcome from (4.21), in which $\bar{H}(\infty) = -0.8845$. This comparison is given in Table 4, in which the numerical results were obtained after both a double Richardson extrapolation in space and time.

TABLE 4

Comparison between numerical and analytical results $H(\infty, t)$ for the intermittently rotating disk flow using the F.I. method.

Time	Numerical	Analytical	Difference
$\pi/32$	−0.8493	−0.8531	0.0038
$\pi/8$	−0.7402	−0.8975	0.1573
$9\pi/32$	−0.6645	–	–
$\pi/2$	−0.6811	–	–
$25\pi/32$	−0.7530	–	–

From this table it is remarkable that there is only agreement for $t = \pi/32$. This was to be expected from (4.21), because of the magnitude of the term of $O(t^3)$ with respect to $H(\infty, t) - \bar{H}(\infty)$. It can be seen that the series is only valid for small values of t.

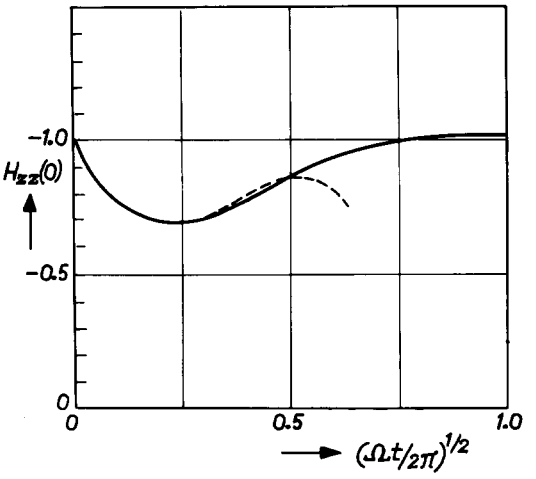

Figure 1. Response of the shear $H_{zz}(0, t)$ to the impulsively altered direction of disk rotation at $t = 0$. ——— numerical, – – – – – (4.20).

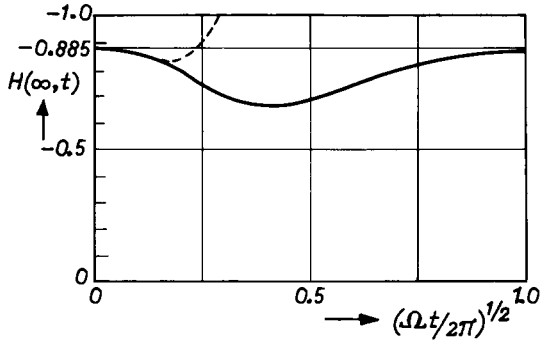

Figure 2. Response of the axial inflow $H(\infty, t)$ to the impulsively altered direction of disk rotation at $t = 0$. ——— numerical, – – – – – (4.21).

The results given in Tables 3 and 4 are displayed in Figures 1 and 2 respectively, in which the scale of time is a quadratic one. It is noteworthy that a new steady state is achieved within about one revolution of the disk. Summarizing it can be concluded that for small values of t the numerical results are in reasonable agreement with the outcome of the analysis.

4.2. Oscillating disk

The problem of a disk performing torsional oscillations at an angular velocity of $\Omega \cos \omega t$ has been studied by Rosenblat [9], Benney [8] and Riley [7]. Rosenblat and Benney have given solutions in the form of asymptotic expansions for the high-frequency case, while Riley considers the low-frequency case too. In Section 4.2.1 we give some results of these papers and extend the work done by Benney. In Section 4.2.2 the numerical results are compared with the outcome of the series expansions.

4.2.1. Analytical results

The basic equations (2.1) – (2.3) are rewritten to make them identical with those of Rosenblat, Benney and Riley. We introduce new coordinates which depend on the parameter $\epsilon = \Omega/\omega$. Putting $t' = \epsilon^{-1}t$ and $z' = (2\epsilon)^{-1/2}z$ this parameter appears in the basic equations. Further let $H(z, t) = -2(2\epsilon)^{1/2}h(z', t')$, $F(z, t) = h_{z'}(z', t')$ and $G(z, t) = g(z', t')$. After substitution and omitting the accents we obtain:

$$h_{zt} = \frac{1}{2}h_{zzz} + \epsilon(2hh_{zz} - h_z^2 + g^2), \tag{4.22}$$

$$g_t = \frac{1}{2}g_{zz} + 2\epsilon(hg_z - h_z g). \tag{4.23}$$

The boundary conditions for h and g are

$$\begin{aligned} &h = h' = 0, \qquad g = \cos(t) \text{ at } z = 0; \\ &h', g \to 0 \text{ for } z \to \infty. \end{aligned} \tag{4.24}$$

We shall first consider the high-frequency case ($\epsilon \ll 1$) and then the low-frequency case ($\epsilon \gg 1$).

(a) High-frequency case ($\epsilon \ll 1$)

Rosenblat has given a solution of (4.22) – (4.23) for small ϵ in the form of series expansions:

$$h(z, t) = \sum_{n=0}^{\infty} \epsilon^n h_n(z, t) \quad \text{and} \quad g(z, t) = \sum_{n=0}^{\infty} \epsilon^n g_n(z, t). \tag{4.25}$$

He shows that $h_0 = g_1 = 0$ and determines h_1, g_0 and g_2 explicitly:

$$g_0(z, t) = e^{-z}\cos(t - z), \tag{4.26}$$

$$\begin{aligned} h_1(z, t) = &-\frac{1}{8}(1 - 2z - e^{-2z}) - \frac{1}{16}\{(2 - \sqrt{2})\cos(2t + \pi/4) + \\ &- 2e^{-\sqrt{2}z}\cos(2t - \sqrt{2}z + \pi/4) + \sqrt{2}e^{-2z}\cos(2t - 2z + \pi/4)\}. \end{aligned} \tag{4.27}$$

Further he calculates the derivative $\partial g_2/(\partial z)$ as:

$$\frac{\partial g_2}{\partial z}(0, t) = -0.060\cos(t) + 0.012\cos(3t) - 0.262\sin(t). \tag{4.28}$$

From (4.27) it can be seen that for large values of z the axial velocity increases linearly with z and the radial component of velocity h_z is not zero, so that the boundary condition $h'(\infty) = 0$ is not satisfied. Riley has shown that the series expansions (4.25) are suitable for describing an oscillatory inner layer near the rotating disk. Outside this layer there is a secondary flow. Using

matched asymptotic expansions Riley was able to find a steady solution representing the first term of an outer expansion. The second time-dependent term can easily be resolved with the multiple scaling technique that Benney used for this problem. He determined series expansions valid throughout the region of flow. The coefficients in the series expansions (4.25) are not only dependent on z and t, but also on $x = \epsilon z$, expressing the dependence on the secondary outer flow. Both Benney and Riley show that h_0 is only zero in the inner layer, but not in the outer layer. It is found that h_0 has to satisfy

$$\begin{aligned} &h_0''' - 2h_0'^2 + 4h_0h_0'' = 0, \\ &h_0(0) = 0, \qquad h_0'(0) = 1/4, \qquad h_0'(\infty) = 0, \end{aligned} \tag{4.29}$$

where the accents denote differentiation with respect to x.

In particular Benney and Riley have calculated:

$$h_0''(0) = -0.207 \quad \text{and} \quad h_0(\infty) = 0.265.$$

Instead of (4.27) Benney finds the following solution for $h_1(z, x, t)$:

$$\begin{aligned} h_1(z, x, t) = a_0 + a_1 e^{-2z} + a_2 \cos(2t + \pi/4) + \\ + a_3 e^{-\sqrt{2}z} \cos(2t - \sqrt{2}z + \pi/4) + a_4 e^{-2z} \cos(2t - 2z + \pi/4), \end{aligned}$$

where $a_0, \ldots, a_4$ are functions of $x = \epsilon z$, for which Benney derived appropriate differential equations and boundary conditions. For verifying our numerical results we are only interested in $h_1(\infty, t)$. From Benney's paper it is easily seen that $a_2 \equiv \frac{1}{16}(\sqrt{2} - 2)$ and we extend his work by determining the function a_0, which follows from

$$a_0''' + 4h_0a_0'' - 4h_0'a_0' + 4h_0''a_0 = 0$$

and

$$a_0(0) = -\frac{1}{8}, \quad a_0'(0) = a_0'(\infty) = 0,$$

where h_0 is equal to the solution of (4.29). In [12] we determined the solution to be

$$a_0(x) = h_0''(0)\{xh_0'(x) + h_0(x)\} - \frac{1}{2}h_0'(x).$$

In particular the axial inflow at infinity is found to be

$$h(\infty, t) = h_0(\infty) + \epsilon\left\{h_0''(0)h_0(\infty) + \frac{1}{16}(\sqrt{2} - 2)\cos(2t + \pi/4)\right\} + O(\epsilon^2). \tag{4.30}$$

(b) Low-frequency case ($\epsilon >> 1$)

The disk slowly changes its direction of rotation. Riley has shown that the main flow is represented by Von Kármán's classical rotating disk solution. He gives a series solution in powers of ϵ^{-1}. In particular, Riley calculates the axial inflow as

$$H(\infty, t) = |\cos(t)|^{\frac{1}{2}} \{-0.88444 + 0.1184\, \epsilon^{-1} \tan(t)/|\cos(t)| + O(\epsilon^{-2})\}. \tag{4.31}$$

This formula is only valid for $\epsilon >> 1$ and not in the neighborhood of a turning point, i.e. $\cos(t) = 0$.

4.2.2. Numerical results

Numerical periodic solutions are obtained for both the high- and low-frequency flow due to an oscillating disk, i.e. in the former case $\epsilon = 0.1$ and in the latter one ϵ takes the values 10 and 100 respectively.

(a) High-frequency case ($\epsilon = 0.1$)

To start our numerical methods we take the state of rest as an initial condition and eliminate the starting effects by calculating a sufficient number of periods. The accuracy of these methods is illustrated by a comparison between the numerical and analytical solutions of the oscillatory boundary layer characterized by the derivative $G_z(0, t)$. We first describe the method used to obtain the numerical results: infinity is fixed at $z_m = 8$ and the range $0 \leqslant z \leqslant 8$ is covered with 80 and 160 uniform meshes successively. In both cases $G_z(0, t)$ is determined by numerical differentiation. In the F.I. method the time step $\Delta t = \epsilon\pi/16, \epsilon\pi/32$, while in the B3 method it is $\epsilon\pi/8$ and $\epsilon\pi/16$. In [12] it was shown that a single Richardson extrapolation can be performed on these results, first in space and then in time. These extrapolations are given in Table 5, together with the outcome of Rosenblat's analytical formulae.

TABLE 5

Comparison between numerical and analytical results for $G_z(0, t)$

Disk velocity	Rosenblat	F.I.	B3
1.0	2.2371	2.2439	2.2394
0.924	1.2138	1.2193	1.2143
0.707	0.0055	0.0087	0.0044
0.383	−1.2041	−1.2035	−1.2067
0.0	−2.2305	−2.2323	−2.2341
−0.383	−2.9170	−2.9220	−2.9212
−0.707	−3.1591	−3.1656	−3.1632
−0.924	−2.9202	−2.9273	−2.9237

Comparing the F.I. and B3 methods we should prefer the latter. In order to get comparable results the F.I. method needs a smaller time step ($\Delta t = \epsilon\pi/32, \epsilon\pi/16$) than the B3 method ($\Delta t = \epsilon\pi/16, \epsilon\pi/8$). For the oscillatory boundary layer problem both methods give results which agree with the analytical solutions. If we want to calculate numerically the outer flow we encounter some difficulties. In the first place the outer flow is a secondary one which is slowly

generated from the state of rest by the oscillatory boundary layer, and hence the numerical results for the outer flow slowly converge. In the second place, Rosenblat shows that the outer boundary layer is of thickness $O(\epsilon^{-1})$ times the thickness of the inner layer. In the case $\epsilon = 0.1$ the inner layer exists in the region $0 \leqslant z < 3$ and therefore it is necessary to fix infinity at $z_m = 32$. If we do not change the number of mesh points, the step size Δz becomes too large in the inner layer. Transforming the z-axis by $z(x) = 8x + 24x^3$ we have a sufficient number of mesh points both in the inner and in the outer layer. In Table 6 we compare the analytical and numerical results obtained with $\Delta x = 1/160$, $\Delta t = \epsilon\pi/16$. The calculations were stopped after the disk had performed 80 periods. In Figure 3 the axial inflow is given as a function of the number of periods. From this figure it can be seen how the outer flow is built up in time. After 80 periods the axial inflow differs about 8% from the analytical solution, represented by the dashed line in Figure 3. This discrepancy is probably mainly due to cutting off the calculations.

TABLE 6

Comparison between analytical and numerical axial inflow, after the disk has performed 80 periods.

Disk velocity	Analytical	Numerical
1.0	−0.231	−0.214
0.924	−0.233	−0.216
0.707	−0.236	−0.219
0.383	−0.237	−0.220
0.0	−0.236	−0.219
−0.383	−0.233	−0.216
−0.707	−0.231	−0.214
−0.924	−0.230	−0.213

From this table we see that the fluctuations in $H(z_m)$ are in good agreement with the time-dependent behaviour of (4.30).

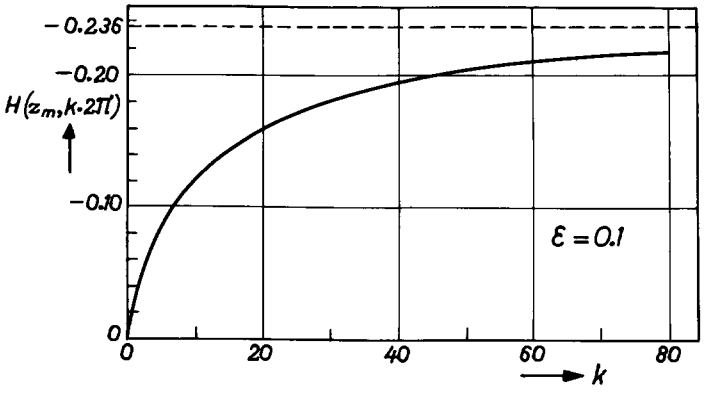

Figure 3. Dependence of the axial inflow $H(\infty, 2k\pi)$ on the number of periods for the high-frequency case $\epsilon = 0.1$. ——— numerical, – – – – – Benney.

(b) Low-frequency case ($\epsilon = 10, 100$)

In this section the numerical results are compared with the outcome of Riley's solution (4.31). We fix infinity at $z_m = 16$ because from Zandbergen and Dijkstra [11] it is known that with this value a sufficiently accurate classical rotating disk solution can be obtained for our application.

In the case $\epsilon = 10$ results were obtained using both the fully implicit and the 3-point backward method. In [12] results are given for $H(z_m, t)$ obtained with $\Delta z = 0.2, 0.1$ and $\Delta t = \epsilon\pi/16$, $\epsilon\pi/32$. After Richardson extrapolation has been applied to these results we infer that the B3 method with the step sizes used produces ≈ 3 significant digits for $H(z_m, t)$. The extrapolations of both methods are given in Table 7, together with the outcome from (4.31).

TABLE 7

Comparison between numerical and analytical results for $H(z_m, t)$ for the case $\epsilon = 10$.

Disk velocity	Riley	F.I.	B3
1.0	−0.8844	−0.9025	−0.8923
0.924	−0.8450	−0.8616	−0.8541
0.707	−0.7296	−0.7556	−0.7483
0.383	−0.5009	−0.5824	−0.5681
0.0	–	−0.3608	−0.3241
−0.383	−0.5933	−0.2863	−0.3062
−0.707	−0.7578	−0.6467	−0.7297
−0.924	−0.8552	−0.8648	−0.8667

Comparing the numerical results of the B3 method with Riley's solution, it is clear that $\epsilon = 10$ is not large enough in the sense of Riley. This is confirmed by the results for $\epsilon = 100$, as shown in Table 8. These numerical results were obtained using the B3 method with $\Delta z = 0.1$ and $\Delta t = \epsilon\pi/32$.

TABLE 8

Comparison between numerical and analytical results for $H(z_m, t)$ for the case $\epsilon = 100$.

Disk velocity	Riley	B3	Disk velocity	Riley	B3
1.0	−0.8844	−0.8837	0.0	–	−0.1917
0.924	−0.8496	−0.8491	−0.383	−0.5517	−0.5466
0.707	−0.7423	−0.7424	−0.707	−0.7451	−0.7451
0.383	−0.5425	−0.5459	−0.924	−0.8506	−0.8500

The dependence of the axial inflow on the angular velocity of the disk is plotted in Figure 4 for the case $\epsilon = 10$. The dashed curve represents Riley's solution (4.31), while the solid curve is an interpolation of the B3 method given in Table 7. The results for the quantities $G_z(0, t)$ and $H_{zz}(0, t)$ are displayed in Figures 5 and 6 respectively.

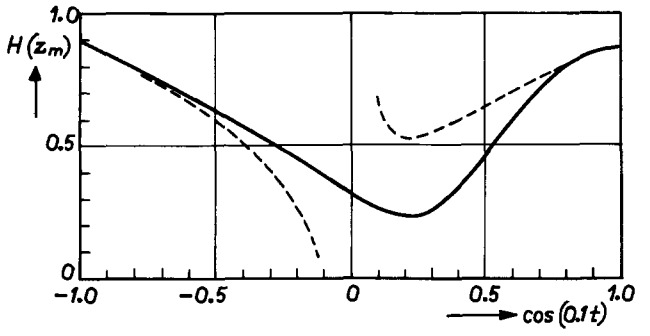

Figure 4. Dependence of the axial inflow $H(\infty, t)$ on the disk velocity in the low-frequency case $\epsilon = 10$. ——— numerical, – – – – – (4.31).

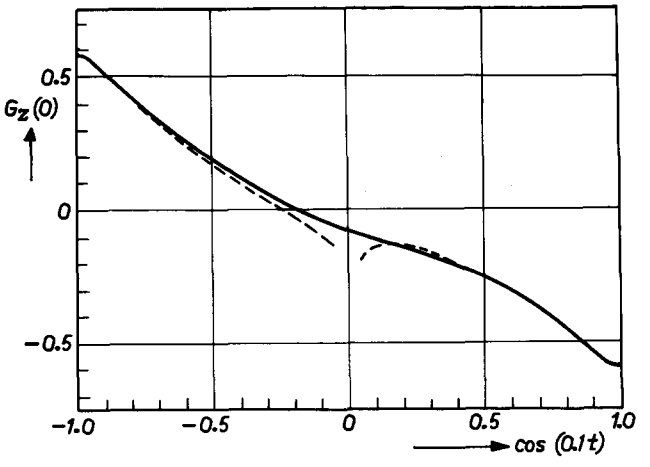

Figure 5. Dependence of the shear $G_z(0, t)$ on the disk velocity ($\epsilon = 10$). ——— numerical, – – – – – Riley.

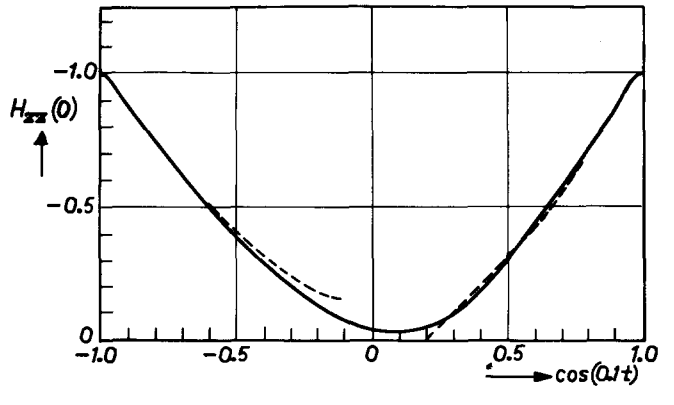

Figure 6. Dependence of the shear $H_{zz}(0, t)$ on the disk velocity ($\epsilon = 10$). ——— numerical, – – – – – Riley.

5. Conclusions

In this paper the time-dependent flow due to an infinite rotating disk has been discussed. Two cases have been considered. In the former case of the intermittently rotating disk the technique of matched asymptotic expansions was successfully used. The formation of the inner expansion runs parallel to the series expansions given by Benton [10]. This approach leads to a hierarchy of ordinary differential equations. After some equations have been solved the difficulty is encountered that the conditions at infinity cannot be fulfilled. This, in fact, makes it necessary to form an outer expansion describing the changing of the outer Von Kármán flow. Just after the reversal of disk rotation the analysis agrees reasonably with the numerical results obtained by using the fully implicit method.

From our investigations on the oscillating disk in an infinite medium we conclude that the three-point backward and fully implicit method produce numerical results which are in good agreement with the analysis given by Rosenblat [9], Benney [8] and Riley [7]. It is also found that the B3 method converges with time one order of magnitude faster than the F.I. method.

In the literature ([4], [11]) multiple solutions to the problems of steadily rotating disk(s) in the Von Kármán class are found. Considering our numerical results we recommend the use of the three-point backward method for investigating the stability of these solutions, which has been performed in [13] for the solution of the single-disk problem.

Acknowledgements

The author whishes to thank the management of the Philips Research Laboratories and of the Mathematical Center for affording him the opportunity of carrying out this research. Furthermore, he would like to express his gratitude to Prof. Dr. P. J. Zandbergen, Dr. H. K. Kuiken and Dr. D. Dijkstra for their guidance.

REFERENCES

[1] C. E. Pearson, A computational method for viscous flow problems, *Journal of Fluid Mechanics*, 21 (1965) 611-622.
[2] C. E. Pearson, Numerical solutions for the time-dependent viscous flow between two rotating coaxial disks, *Journal of Fluid Mechanics*, 21 (1965) 623-633.
[3] P. Florent, N. D. Nguyen & N. D. Vo, Ecoulement instationaire entre disques coaxiaux, *Journal de Méchanique*, 12 (1973) 555-580.
[4] N. D. Nguyen, J. P. Ribault & P. Florent, Multiple solutions for flow between coaxial disks, *Journal of Fluid Mechanics*, 68 (1975) 369-388.
[5] R. J. Bodonyi & K. Stewartson, The unsteady laminar boundary layer on a rotating disk in a counter-rotating fluid, *Journal of Fluid Mechanics*, 79 (1977) 669-688.
[6] G. M. Homsy & J. L. Hudson, Transient flow near a rotating disk, *Applied Scientific Research*, 18 (1968) 384-397.
[7] N. Riley, Oscillating viscous flows, *Mathematika*, 12 (1965) 161-175.
[8] D. J. Benney, The flow induced by a disk oscillating in its own plane, *Journal of Fluid Mechanics*, 18 (1964) 385-391.
[9] S. Rosenblat, Torsional oscillations of a plane in a viscous fluid, *Journal of Fluid Mechanics*, 5 (1959) 206-220.
[10] E. R. Benton, On the flow due to a rotating disk, *Journal of Fluid Mechanics*, 24 (1966) 781-800.

[11] P. J. Zandbergen & D. Dijkstra, Non-unique solutions of the Navier-Stokes equations for the Kármán swirling flow, *Journal of Engineering Mathematics*, 11 (1977) 167-188.

[12] H. Schippers, Time dependent flow due to an infinite rotating disk, Memorandum 214, Department of Applied Mathematics, Twente University of Technology, Enschede, The Netherlands.

[13] D. Dijkstra, H. Schippers & P. J. Zandbergen, On certain solutions of the non-stationary equations for rotating flow, *Proc. 6th International Conference on Numerical Methods in Fluid Dynamics* (Tbilisi, 1978). (To be published, Springer-Verlag, Berlin).